

Propagation of Initially Excited States in Time-Dependent Density Functional Theory

Peter Elliott and Neepa T. Maitra

*Department of Physics and Astronomy, Hunter College and the City
University of New York, 695 Park Avenue, New York, New York 10065, USA*

Many recent applications of time-dependent density functional theory begin in an initially excited state, and propagate it using an adiabatic approximation for the exchange-correlation potential. This however inserts the excited-state density into a ground-state approximation. By studying a series of model calculations, we highlight the relevance of initial-state dependence of the exact functional when starting in an excited state, and explore the errors inherent in the adiabatic approximation that neglect this dependence.

I. INTRODUCTION

Time-dependent density functional theory (TDDFT) is an exact reformulation of the time-dependent quantum mechanics of many-electron systems [1, 2] that operates by mapping a system of interacting electrons into one of fictitious non-interacting fermions, the Kohn-Sham (KS) system, reproducing the same time-dependent density of the true system. By the theorems of TDDFT, all properties of the true interacting system may be obtained from the KS system, in principle. In practice, approximations are needed for the exchange-correlation effects: in particular, for the exchange-correlation (xc) potential, $v_{xc}[n; \Psi(0), \Phi(0)](\mathbf{r}, t)$, a crucial term in the single-particle KS equations determining the evolution of the fictitious non-interacting fermions. This functionally depends on the one-body density, $n(\mathbf{r}, t)$, the initial many-body state of the interacting system $\Psi(0)$, and the initial state of the KS system $\Phi(0)$.

From the inception of the theory, subtleties were noted in the functional-dependences, which make good approximations for the xc potential more challenging to derive than for its counterpart in the (much older) ground-state density functional theory [3–5]. One of these is memory: the dependence of the potential at time t on the density at earlier times, and on the initial-states $\Psi(0)$ and $\Phi(0)$. Efforts to include memory-dependence in functionals [6–14], are not widely used, and have all focussed on the dependence on the history of the density, neglecting the dependence on the initial states. The vast majority of applications have been in linear response from a non-degenerate ground-state, and there this initial-state dependence (ISD) is redundant: by the Hohenberg-Kohn theorem, a non-degenerate ground-state is a functional of its own density. In fact, the simple adiabatic approximation, where the instantaneous density is input into a ground-state approximation, neglecting any memory-dependence, has shown remarkable success for a great range of excitations and spectra. All commonly available codes with TDDFT capabilities are written assuming the adiabatic approximation. Over the years it has been understood that certain types of excitations cannot be captured by the adiabatic approximation, e.g. double excitations [15], excitonic series in optical response of semiconductors [16], and there is both

on-going research in developing frequency-dependent kernels to deal with this, as well as understanding when not to trust the calculated adiabatic TDDFT spectra.

With the results and understanding of recent years lending a level of comfort with calculations of spectra and response, TDDFT has now entered a more mature stage, and with that, comes more adventurous applications. In particular, for electron dynamics in real time, evolving under strong laser fields, or coupled electron-nuclear dynamics following photo-excitation (e.g. Refs. [17–19]). The role of memory is less well-understood in these applications; studies on model systems have shown that sometimes memory-dependence is essential [20–24], other times it is not important at all [25, 26]. Moreover a new element enters: the initial-state dependence that was conveniently and correctly brushed aside in the linear response regime, now raises its head. In applications such as modeling solar cell processes, the initial photo-excitation of the electronic system is not dynamically modeled; instead the dynamics begins with the electronic system assumed to be in an excited state. The initial state is not the ground-state, yet no truly initial-state dependent functionals are available today, hence we ask how large are the errors in such calculations? Knowing that the true interacting system begins in a certain excited state, is there an optimal choice for the initial KS state when propagating with an adiabatic approximation? How large are the errors due to ISD compared to those due to history-dependence?

In this paper, we begin to answer these questions by considering a series of model calculations of two-electron systems. We start by reviewing the underlying theorems of TDDFT and the subtleties of ISD, even in situations where we may not expect it. We show how ISD leads to a non-zero xc potential even for non-interacting electrons.

Then, we move to electron dynamics in the model soft-Coulomb helium atom, performing adiabatic TDDFT calculations with different initial-states and comparing with exact dynamics. Here we must dissect other sources of error in usual TDDFT calculations, such as using an initial KS excited state whose density does not equal the true excited state density, in order to properly ascribe the influence of ISD. Finally we make the first step towards investigating how ISD

can affect an area currently of much interest, namely coupled electron-ion dynamics, by performing Ehrenfest calculations for a model LiH system. We work in atomic units throughout ($e^2 = m_e = \hbar = 1$).

II. INITIAL-STATE DEPENDENCE IN TDDFT

In TDDFT, one evolves a set of single-particle orbitals $\{\phi_j(\mathbf{r}, t)\}$ with a one-body KS potential:

$$i\frac{\partial}{\partial t}\phi_j(\mathbf{r}, t) = \left(-\frac{1}{2}\nabla^2 + v_s(\mathbf{r}, t)\right)\phi_j(\mathbf{r}, t) \quad (1)$$

$$v_s(\mathbf{r}, t) = v_{\text{ext}}(\mathbf{r}, t) + v_{\text{xc}}[n](\mathbf{r}, t) + v_{\text{xc}}[n; \Psi_0, \Phi_0](\mathbf{r}, t) \quad (2)$$

where $v_H(\mathbf{r}, t) = \int n(\mathbf{r}', t)/|\mathbf{r}-\mathbf{r}'|d^3r'$ is the usual Hartree potential and $v_{\text{xc}}(\mathbf{r}, t)$ is the xc potential which depends on the entire history of the density, the interacting initial state Ψ_0 , and the initial KS wavefunction Φ_0 .

The origin of the initial-state dependence in the functionals is that the one-to-one Runge-Gross mapping [1] between time-dependent densities and potentials holds for a fixed initial-state. Thus, the external potential v_{ext} functionally depends on the density and the true initial state $\Psi(0)$, and the KS potential v_s depends on the density and the KS initial state $\Phi(0)$. These functional dependences are not directly relevant themselves in a practical calculation, because there only the xc potential v_{xc} needs to be approximated. However, they lend their dependences to v_{xc} via Eq. (2), which must therefore depend on both initial states and the density.

There are two known situations in which there is no initial-state dependence. When the initial state is a ground-state, then, by the Hohenberg-Kohn theorem of ground-state DFT, it is itself a functional of its own density. ISD is redundant, as the information about the initial state is contained in the initial density. (See also Sec. II A). The other situation is for one-electron systems: starting in *any* initial state, there is only one potential that can yield a given density-evolution [27]. In all other situations, it is assumed that ISD cannot be subsumed into a density-dependence; explicit demonstrations for two electrons can be found in Refs. [22, 27]. Ref. [28] derived an exact condition relating the dependence on the history of the density to ISD. This condition is likely violated by any history-dependent functional approximation that has no ISD.

Technically, one may choose any initial KS wavefunction that has the same n and \dot{n} as the true initial state [29]. Usually a single Slater-determinant of N spin-

orbitals ϕ_i is selected, with the required property that

$$\sum_{i=1}^N |\phi_i(\mathbf{r}, 0)|^2 = n(\mathbf{r}, 0) \text{ and} \quad (3)$$

$$-\nabla \cdot \text{Im} \sum_{i=1}^N \phi_i^*(\mathbf{r}, 0) \nabla \phi_i(\mathbf{r}, 0) = \dot{n}(\mathbf{r}, 0) \quad (4)$$

where

$$n(\mathbf{r}, 0) = N \sum_{\sigma} \int dx_2 \cdots \int dx_N |\Psi(x, x_2 \cdots x_N, 0)|^2 \quad (5)$$

$$\dot{n}(\mathbf{r}, 0) = -N \nabla \cdot \text{Im} \left\{ \sum_{\sigma} \int dx_2 \cdots \int dx_N \Psi^*(x, x_2 \cdots x_N, 0) \nabla \Psi(x, x_2, \cdots, x_N, 0) \right\} \quad (6)$$

where $x = (\mathbf{r}, \sigma)$ and $\int dx = \sum_{\sigma} \int d^3x$.

In this paper we will consider different choices of $\Phi(0)$ for two-electron systems that begin in the first excited singlet state of the true system, denoted Ψ^* . Specifically we will, at various points, investigate the following three forms:

(a) An excited KS singlet state with two occupied orbitals ϕ_0 and ϕ_1 , whose spatial part has the form

$$\Phi^*(\mathbf{r}_1, \mathbf{r}_2) = \frac{1}{\sqrt{2}} (\phi_0(\mathbf{r}_1)\phi_1(\mathbf{r}_2) + \phi_0(\mathbf{r}_2)\phi_1(\mathbf{r}_1)) \quad (7)$$

Note that this state is a sum of two Slater determinants.

(b) A ground KS singlet state, Φ^{gs} , which, for two electrons corresponds to a single doubly-occupied orbital

$$\Phi^{\text{gs}}[n^*](\mathbf{r}_1, \mathbf{r}_2) = \phi(\mathbf{r}_1)\phi(\mathbf{r}_2), \quad (8)$$

with

$$\phi(\mathbf{r}) = \sqrt{n^*(\mathbf{r})/2} \quad (9)$$

where $n^*(\mathbf{r}) = 2 \int |\Psi^*(\mathbf{r}, \mathbf{r}')|^2 d^3r'$ is the density of the initial excited state. This is a single Slater-determinant, and is the usual choice when the true initial state is a ground state.

(c) A spin-symmetry-broken excited KS state of the form

$$\Phi_{\text{SB}}^*(\mathbf{r}'\sigma', \mathbf{r}\sigma) = \frac{1}{\sqrt{2}} \begin{vmatrix} \phi_0(\mathbf{r})\delta_{\sigma\uparrow} & \phi_0(\mathbf{r}')\delta_{\sigma'\uparrow} \\ \phi_1(\mathbf{r})\delta_{\sigma\downarrow} & \phi_1(\mathbf{r}')\delta_{\sigma'\downarrow} \end{vmatrix} \quad (10)$$

This state is not a spin-eigenstate (although it does have $\langle S \rangle = 0$), but is a valid choice for an initial KS state, having the same total density as the true system. The up and down spin-densities are not equal, and we shall evolve them in different spin-up and spin-down KS potentials, but, unlike in spin-DFT, we do not consider the spin-

densities separately meaningful; only their sum is considered as an observable [30]. Instead, (c) will be used to illustrate the effects of orbital-specific functionals, as will be discussed more later.

Now the exact KS potential differs depending on which choice (a), (b), or (c), is made, but any adiabatic approximation is identical for them all. Almost all the calculations being run today, certainly all that are coded in the commonly available codes, utilize such an approximation, and insert the instantaneous density into a ground-state approximation:

$$v_{xc}^{\text{adia}}[n; \Psi(0), \Phi(0)](\mathbf{r}, t) = v_{xc}^{\text{gs}}[n(t)](\mathbf{r}). \quad (11)$$

It is not surprising that there are errors inherent in such an approximation but one question we hope to shed light on by our investigations here, is how much of this error is due to the lack of ISD, rather than the lack of history-dependence (dependence on $n(\mathbf{r}, t' < t)$). Only the latter occurs in usual calculations that begin in an initial ground-state, where, as mentioned earlier, ISD may be subsumed into density-dependence.

A. Beginning in the ground-state: ISD or not?

Many practical situations start with the system in its ground-state; in fact most calculations, except in the most recent years, have assumed an initial ground-state. This is fortunate for TDDFT, since, at least at short times, the adiabatic approximation with its ground-state functionals, which have become increasingly sophisticated over the years, could then be expected to work reasonably well. However, we will show that the subtleties of initial-state dependence can appear even in this case.

A completely legitimate choice for the KS initial state would be the true ground-state wavefunction as it trivially satisfies the initial conditions Eq. (3) and Eq. (4). The exact KS potential, for this choice, reproduces the density evolution of the exact wavefunction propagating in the interacting system by propagating the exact wavefunction in a non-interacting system.

Given that at the initial time we are dealing with a ground-state, one might expect that the adiabatic approximation would be exact, at least initially, however this is not the case. The adiabatic approximation returns the xc potential for a ground-state DFT calculation, where the KS wavefunction is the ground-state KS wavefunction. If we were to start the KS calculation with this ground-state KS wavefunction, the adiabatic approximation is then exact at the initial time.

However the initial interacting wavefunction is not a ground state of the non-interacting KS system, and so, choosing this as the initial KS state means the adiabatic approximation will be in error from the start.

Thus care must be taken when using the short-hand that there is no initial-state dependence when starting in the ground-state. More precisely, what is meant is that

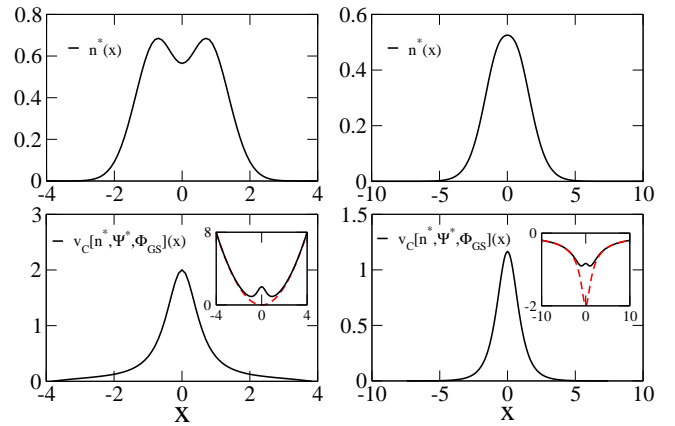


FIG. 1: Top Panels: The first excited-state density, $n^*(x)$, for two non-interacting electrons in a one-dimensional harmonic potential (left) and soft-Coulomb potential (right). Lower Panels: The corresponding correlation potentials, $v_c[n^*, \Psi^*, \Phi_{\text{gs}}^{\text{gs}}](x)$, for an initial KS wavefunction chosen to have ground-state form but yielding the initial excited-state density n^* (case (b) of text). The insert shows the KS potential (solid line) compared with the external potential (dashed line), chosen as harmonic and soft-Coulomb, respectively. When the initial KS state is chosen to be Φ^* (case (a) in text), on the other hand, the correlation potential is zero.

1) the initial KS orbitals are chosen to be those of the KS ground-state wavefunction, and 2) the dependence on initial state for this case can be subsumed into the density via the theorems of ground-state DFT.

III. NON-INTERACTING ELECTRONS

The importance of initial-state dependence is strikingly evident even for the hypothetical case of non-interacting electrons. Due to ISD, the xc potential is *not* always equal to zero, which may be surprising at first sight, given that there is no interaction. Although no-one in their right mind would perform KS calculations for non-interacting electrons for practical purposes, it is instructive to consider how the KS system behaves in this case. In particular, the studies suggest what is the best choice of KS initial state for a given true initial state when an adiabatic approximation is used. Since the adiabatic approximation is designed for ground-states, is the error least if we always choose a KS state that is a ground-state?

In the following we consider the “true” system to be non-interacting, i.e. we scale the electron-electron interaction by λ in the limit that $\lambda \rightarrow 0$ and consider terms zero-th order in λ only, e.g. the Hartree potential vanishes. We then consider the xc potential when the KS system is started in different allowed initial-states.

Consider two non-interacting electrons prepared in an excited state Ψ^* and evolving in some potential $v_{\text{ext}}(t)$. To start the KS evolution, any initial state of the

same density n , and first time-derivative, \dot{n} , zero in this case, may be chosen. We consider the initial state choices (a) and (b) introduced in Sec. II, which become here: (a) $\Phi(0) = \Psi^*$, and (b) $\Phi(0) = \phi_0(\mathbf{r})\phi_0(\mathbf{r}') = \Phi^{\text{gs}}$, $\phi_0 = \sqrt{n^*/2}$, where n^* is the density of Ψ^* .

For choice (a), the exact xc potential vanishes, $v_{\text{xc}}[n; \Psi^*, \Phi^*](\mathbf{r}, t) = 0$. This can be most easily seen by invoking the uniqueness property of the Runge-Gross mapping: for a fixed particle-interaction, only one potential ($v_{\text{ext}}(t)$) can yield a given density-evolution from a given initial state. Since $\Phi^* = \Psi^*$ for choice (a), we conclude $v_{\text{xc}}(t) = 0$. This result can also be seen from the general formula [29]:

$$\nabla \cdot [n(\mathbf{r}, t) \nabla (v_{\text{H}}(\mathbf{r}, t) + v_{\text{xc}}(\mathbf{r}, t))] = q(\mathbf{r}, t) - q_{\text{s}}(\mathbf{r}, t) \quad (12)$$

where

$$q(\mathbf{r}, t) = \frac{1}{i\hbar} \nabla \cdot \langle \Psi(t) | [\hat{\mathbf{j}}(\mathbf{r}), \hat{T} + \hat{V}_{\text{ee}}] | \Psi(t) \rangle \quad (13)$$

$$q_{\text{s}}(\mathbf{r}, t) = \frac{1}{i\hbar} \nabla \cdot \langle \Phi(t) | [\hat{\mathbf{j}}(\mathbf{r}), \hat{T}] | \Phi(t) \rangle \quad (14)$$

and $\hat{\mathbf{j}}(\mathbf{r})$ is the current-density operator. When the two initial wavefunctions are the same, the RHS vanishes at $t = 0$ in the non-interacting limit, and we are left with $v_{\text{H}}(t = 0) = 0$, and $v_{\text{xc}}(t = 0) = 0$. Stepping forward in time, it follows that $v_{\text{xc}}(t) = 0$ for all times.

Now consider choice (b). In this case, $v_{\text{xc}}[n; \Psi^*, \Phi^{\text{gs}}](\mathbf{r}, 0)$ is non-zero: the RHS of Eq. (12) at $t = 0$ is no longer zero in the non-interacting limit, due to the difference in the initial wavefunction in q and q_{s} . That this is non-zero is also expected by the fact that v_{xc} must be such that $v_{\text{s}} = v_{\text{ext}} + v_{\text{Hxc}}$ evolves the initial Φ^{gs} with the same density for all time as the different initial state Ψ^* has when evolved in v_{ext} . So, ISD leads to a non-zero xc potential, even when the electrons do not interact.

For an explicit demonstration, consider the initial time and realize that $v_{\text{xc}}(t = 0)$ depends entirely on the initial states, as can be seen from Eq. (12), and not on the choice of the external potential. Figure 1 plots this potential $v_{\text{xc}}(t = 0)$ for the first excited state of an external harmonic potential ($\frac{1}{2}x^2$, on the left), and a soft-Coulomb potential ($-2/\sqrt{x^2 + 1}$, on the right) in one-dimension. The top panels show the density, and the insets show the external potential in which Ψ^* is an eigenstate, as well as the KS potential $v_{\text{ext}} + v_{\text{c}}$ in which Φ^{gs} is an eigenstate (the ground-state, since there are no nodes). Because for two electrons in a spin-singlet with one doubly-occupied orbital, $v_{\text{x}} = -v_{\text{H}}/2 = 0$ in the non-interacting limit, this effect appears entirely in the correlation potential, and can be interpreted as *static correlation*: due completely to the non-single-determinantal structure of the true initial state. In case (a), this effect vanishes, because the KS initial state is chosen also not to be a SSD.

We now ask what an adiabatic potential would give:

approximating $v_{\text{xc}}[n; \Psi(0), \Phi(0)]$ by a ground-state potential $v_{\text{xc}}^{\text{gs}}[n]$. To distinguish errors arising from the choice of approximate ground-state functional itself, we consider an “adiabatically exact” potential [21, 25], $v_{\text{xc}}^{\text{adia-ex}}[n]$. We shall define this generally in the next section, but for now it suffices to define it such that if both the true and KS wavefunctions at all times were in fact ground states of some potential, then the exact xc potential is the exact ground-state one, $v_{\text{xc}}[n; \Psi^{\text{gs}}, \Phi^{\text{gs}}] = v_{\text{xc}}^{\text{adia-ex}}[n]$. Consider again just the initial time, $t = 0$. In the non-interacting limit, for both the true and KS wavefunctions to be ground-states that have the density of the excited state Ψ^* , then $\Psi(0) = \Phi(0) = \sqrt{n_0(\mathbf{r})n_0(\mathbf{r}')}/2$, and we rapidly conclude that

$$v_{\text{xc}}[n, \Psi^{\text{gs}}, \Phi^{\text{gs}}](\mathbf{r}, t) = v_{\text{xc}}^{\text{adia-ex}}[n](\mathbf{r}, t) = 0 \quad (15)$$

in the non-interacting limit. Applying now this adiabatic approximation to the case of the initial true excited state Ψ^* considered above, we conclude that *the adiabatic approximation is exact for choice (a)*, when the initial KS state is also chosen excited, as we had argued there the exact v_{xc} also vanishes. It is inaccurate for choice (b), when the initial KS state is chosen to be a ground-state one, where the exact correlation potential is non-zero.

This study suggests that in the general interacting case, errors in adiabatic TDDFT will be least when an initial KS state that most closely resembles the configuration of the true excited state is chosen. This expectation is indeed borne out in the following studies.

IV. MODEL TWO-ELECTRON SOFT-COULOMB INTERACTING SYSTEMS

The case of non-interacting electrons illustrated the importance of ISD, while offering a hopeful diagnosis for the adiabatic approximation; the latter becomes exact if the initial state is chosen appropriately. Of course, electrons do interact, and now we turn to studying the effect of ISD on the dynamics of interacting systems.

When running an approximate TDKS calculation starting in an excited state of the interacting problem, three separate sources of error come into play. First, excited states of the exact ground-state KS potential $v_{\text{s}}[n_0](\mathbf{r})$ do not have the same densities as interacting excited states of the potential $v_{\text{ext}}(\mathbf{r})$ whose ground-state density is $n_0(\mathbf{r})$. Yet these are usually the ones chosen in practice. We discuss this problem in Section IV A. The second source of error is the central one for this paper: the use of the adiabatic approximation, when, from the start, we have an excited state. We consider first the “adiabatically exact” approximation, mentioned also in Sec. III, but considered now for interacting electrons, in Section IV B. This will allow us to separate the errors from the choice of ground-state functional approximation used in the adiabatic approximation, which is the

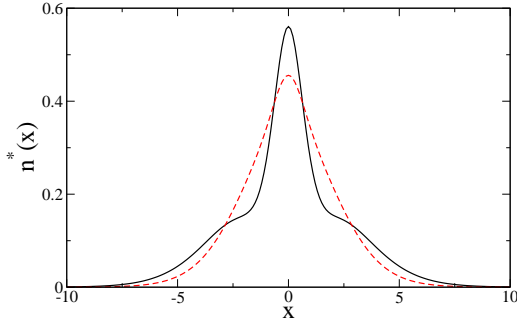


FIG. 2: Exact excited-state density (solid line) compared to the exact excited-state density of the exact ground-state KS potential (dashed line) for the soft-Coulomb Helium atom.

third issue. In Sections IV D, and V, we will study the effect that missing initial-state dependence has in practice, on electron dynamics in model two-electron systems when begun in the first singlet excited state of the system.

In our model one-dimensional Helium atom, the two electrons interact via a soft-Coulomb electron-electron interaction, $v_{ee}(x_1, x_2) = 1/\sqrt{(x_1 - x_2)^2 + 1}$ and live in an external soft-Coulomb potential,

$$v_{\text{ext}}(x) = -2/\sqrt{x^2 + 1}. \quad (16)$$

Such a model, straightforward to solve numerically, is popular in understanding and analyzing electron interactions, in both the ground-state and in strong-field dynamics [31], inside and outside the density-functional community. In our model of the diatomic LiH molecule, the soft-Coulomb interaction is also used, while the external potential has an asymmetric soft-Coulomb well structure (Sec. V).

Before proceeding, we make a computational note. The true dynamics are propagated on a real-space grid using the exponent midpoint rule Taylor-expanded to fourth order. Imaginary time propagation along with Gram-Schmidt orthogonalisation is first performed to find the lowest eigenstates. The adiabatic exact-exchange (AEXX) dynamics uses the Crank-Nicolson method with an explicit predictor step for the Hartree-exchange potential. In both cases, a timestep of 0.001 is used with a grid spacing of 0.1. When possible these calculations were tested for accuracy against the parallelized code OCTOPUS[32], which was also used for LDA and LDA-SIC runs.

A. The Excited-State Density

The theorems of TDDFT require that the KS initial state has the same $n(\mathbf{r}, 0)$ and $\dot{n}(\mathbf{r}, 0)$ as the true interacting system (Sec. II). In this section we discuss the difficulty of fulfilling this requirement when the initial state is not a ground-state.

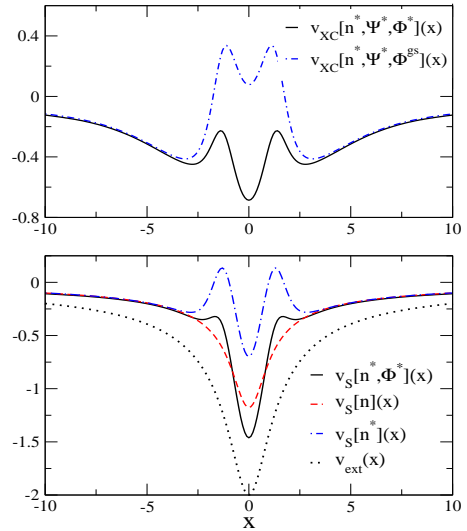


FIG. 3: Top Panel: The exact xc potentials for the two choices of initial state, Φ^* (solid line) and Φ^{gs} (dot-dashed line). Lower Panel: The KS potentials for which the two initial state choices, Φ^* (solid line) and Φ^{gs} (dot-dashed line) are eigenstates. Also shown are the exact ground-state KS potential (dashed line) for the soft-Coulomb Helium potential (dotted line).

When the true initial state is a ground-state, the natural and usual choice for the KS initial state is the non-interacting ground-state, and this can be found by solving the ground-state KS equations. However, if we want to compute the dynamics of an excited state, we encounter the problem that there is no DFT scheme to find excited state densities[34]. Furthermore, even if we use a more computationally expensive higher-level wavefunction method to calculate the state $\Psi(0)$, we still must then choose an initial $\Phi(0)$ in which to start the KS calculation. If we start the interacting system in a first excited state of some $v_{\text{ext}}(\mathbf{r})$, the results of the earlier sections suggest a good choice for adiabatic TDDFT is to start the KS system in a corresponding non-interacting excited state where one electron is excited from the highest occupied to lowest unoccupied orbital of some \tilde{v}_s (as in form (a) of Sec. II). This $\tilde{v}_s(\mathbf{r})$ however cannot be the ground-state KS potential $v_s(\mathbf{r})$ corresponding to the interacting v_{ext} , because this would not satisfy Eq. (3): $v_s(\mathbf{r})$ yields the same ground-state density in a non-interacting system that $v_{\text{ext}}(\mathbf{r})$ yields in the interacting one, but the densities of their excited-states are different. Yet, the usual practice is to use the corresponding excited-state of the ground-state KS potential [33]. This is partly because the density of the interacting excited state is not often known anyway. In Fig. 2 we compare the exact density of the first excited interacting singlet state in the soft-Coulomb He atom (Eq. 16) with the density of the excited state of the corresponding ground-state KS potential. Although matching the general shape, the latter is too narrow and misses some structure.

To be able to separate the error from not quite having the exact initial density from the error from using an adiabatic approximation, we now search for a non-interacting system where the first singlet excited-state density is exactly equal to the true excited-state density n^* , for our model He atom. Several such potentials may exist [34], and in the lower panel of Fig. 3, we plot one such KS potential, denoted $v_s[n^*, \Phi^*](x)$ and compare to the KS potential where $n(x)$ is the exact ground-state density $v_s[n](x, 0)$ of the model He atom. (The first excited state densities of these potentials are precisely those shown in Fig. 2). We also show $v_s[n^*](x, 0)$, i.e. the KS potential for which $n^*(x)$ is the density of the ground-state. This corresponds to choice (b) in Sec. II for the initial KS state.

Once a valid KS state is found satisfying Eqs. (3) and (4), the initial xc potential is completely determined: Eqs. (12) and (13) show that at the initial time, v_{xc} is a functional of just the two initial states $\Psi(0)$ and $\Phi(0)$. This can be added to any external potential, prescribed by the physical problem at hand, and Hartree-potential, determined by the initial density, to start the evolution. In other words, the choice of the initial KS state fundamentally points to an xc potential, rather than to a KS potential, and so in the top panel of Fig. 3 we plot the xc potentials corresponding to choices (a) and (b) of the initial KS state. In the following examples, we take the initial v_{ext} to be that of the soft-Coulomb Eq. (16); sometimes subsequently an external field is added.

We have therefore, now found initial states of the form (a) and (b) of Sec II, both yielding the same density as that of the true excited-state, meeting the conditions Eq. (3) and (4). We can now move forward to investigate the time-dependent properties.

B. The Exact Adiabatic Approximation

We next move to the error introduced by using the adiabatic approximation.

To isolate this error we will calculate the adiabatically exact potential at the initial time, and start in a KS state of the exact same density as the true state, as found in Section IV A.

The adiabatically exact potential is defined by [25]

$$v_{xc}^{\text{adia-ex}}[n] = v_s^{\text{adia-all}}[n] - v_{\text{ext}}^{\text{adia-all}}[n] - v_H[n] \quad (17)$$

where $v_s^{\text{adia-all}}[n](\mathbf{r}, t)$ is the potential for which $n(\mathbf{r}, t)$ is the non-interacting ground state density and $v_{\text{ext}}^{\text{adia-all}}[n](x)$ is the potential for which interacting electrons have $n(\mathbf{r}, t)$ as their ground-state density. If both the true and KS wavefunctions are actually always in some ground-state, then Eq. (17) becomes the exact xc potential. We shall consider this potential for initially excited states, only at the initial time.

The non-interacting potential $v_s^{\text{adia-all}}[n^*](\mathbf{r}, 0)$ may be easily found by inverting the KS equation for a

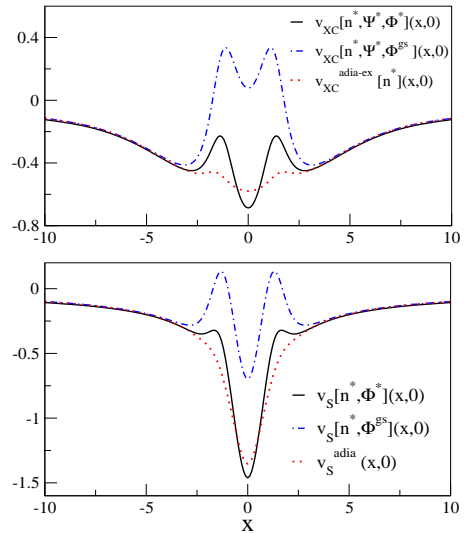


FIG. 4: Top Panel: The exact xc potentials and the exact adiabatic xc potential. Lower Panel: The exact and adiabatically-exact KS potentials.

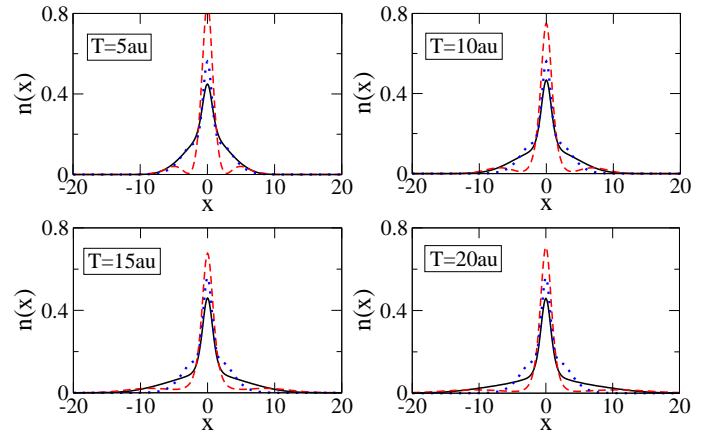


FIG. 5: The density at times 5au, 10au, 15au, and 20au for initial states Φ^* (solid line) and Φ^{gs} (dashed line) propagating in the static exact-adiabatic initial potential. Also shown is the exact excited-state density (dotted line) which is the exact solution at each time.

doubly-occupied orbital, $\phi(\mathbf{r}) = \sqrt{n^*(\mathbf{r})/2}$ where $n^*(\mathbf{r})$ is the density of the initial state Ψ^* .

The interacting potential, $v_{\text{ext}}^{\text{adia-all}}[n](\mathbf{r}, 0)$ is solved for using an iterative technique whereby the external potential is updated based on the difference between the ground-state density of the current iteration and the density we are targeting. This is based on the inversion algorithm of Ref. 35, but generalized to the interacting case[25]. We also increase the update to the potential in regions of low density by simply using the inverse of the density (up to a maximum value) as a weighting factor, similar to Ref. 30. When the density converges to the target density, we have found $v_{\text{ext}}^{\text{adia-all}}[n](x)$.

The dotted line in the lower panel of Fig. 4, shows at the initial time, the full KS potential with the adiabatically exact xc potential, namely $v_s^{\text{adia}}(x) = v_{\text{ext}}(x) + v_H[n](x) + v_{\text{xc}}^{\text{adia-ex}}[n](x)$, choosing $v_{\text{ext}}(t=0)$ as the soft-Coulomb potential of Eq. 16, for the first excited singlet state Ψ^* . Alongside, we compare this to the exact KS potentials found in Sec. IV A (see Fig. 3), for the initial state choices of case (a) and (b) respectively. The adiabatically exact KS potential $v_s^{\text{adia}}(x)$ tracks the shape of the exact KS potential $v_s[n^*, \Psi^*, \Phi^*]$ although misses structure. The difference between them is the difference in their xc potentials shown in the upper panel of Fig. 4. The difference is much larger for the comparison with the exact KS potential when the initial KS state is chosen as the ground-state, (i.e. $v_{\text{xc}}^{\text{adia-ex}}[n^*]$ is closer to $v_{\text{xc}}[n^*, \Psi^*, \Phi^*]$ than it is to $v_{\text{xc}}[n^*, \Psi^*, \Phi^{\text{gs}}[n^*]]$); in this case, there is a large static-correlation contribution to the exact xc potential. The results here are consistent with the non-interacting case discussed in Sec. III: with interaction, the adiabatic approximation is no longer exact for the choice of Φ^* , however it is still the better choice over Φ^{gs} .

The fact that the adiabatically exact potential does not equal the true potential, even at the *initial* time, leads to erroneous dynamics. To illustrate this effect we propagate our exact initial wavefunctions in the adiabatically exact potential and compare with exact dynamics. Since calculating at each time is computationally demanding and delicate, we will simply evolve in time without any additional perturbing potentials, and hold the adiabatic potential fixed to its initial value. The idea is that since the exact evolution is static, the adiabatically exact potential is static and equals its initial value at all times; if this was a good approximation, it would yield density-dynamics that were close to static. The deviation of the adiabatic propagation from the exact is a measure of its error. Note such a calculation does not treat the adiabatic potential self-consistently; later calculations with approximate adiabatic functionals suggest having self-consistency decreases the error somewhat.

In Fig. 5, we plot snapshots of the density at 5au intervals until $T = 20\text{au}$ for the two choices of exact initial states discussed above, evolving in the fixed adiabatically exact potential plotted in Fig. 4. As each time we show the exact static excited-state density. While both choices show density ‘leaking’ out, the Φ^* choice is more successful in preventing this, as might be expected from the above discussions, but cannot stop the density melting away in its outer regions. The $\Phi^{\text{gs}}[n^*]$ choice is poor from the start, jettisoning density outwards and becoming too narrow.

This error in the adiabatically exact evolution is caused *entirely* by initial-state dependence: for the analogous calculation beginning in the interacting ground-state and starting with the ground-state KS wavefunction, the adiabatic approximation would be exact at all times when there are no perturbing fields.

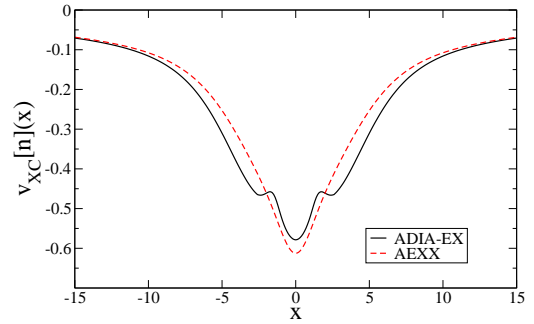


FIG. 6: The exact adiabatic xc (solid) and AEXX (dashed) potentials evaluated on the true excited-state density n^* . (Note that the solid line here is the same as the dotted line in the top panel of Fig. 4)

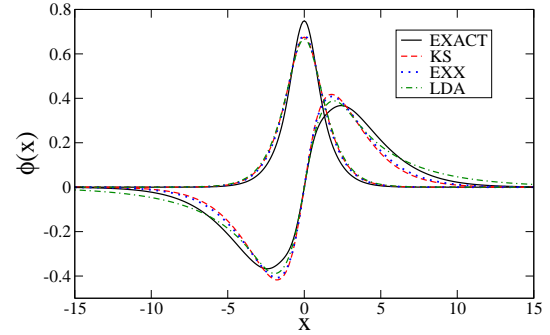


FIG. 7: The ground and first excited orbitals from ground-state EXX and LDA, compared to those from the exact GS KS potential. Also shown are those orbitals found in Sec. IV A of this configuration that yield the exact excited-state density.

C. Approximate GS functionals

Finally we look at the third source of error, namely using an approximate ground-state xc functional instead of the exact one. This error contributes at both the ground-state level in obtaining the initial orbitals, and in the adiabatic functional when computing dynamics. We first turn our attention to the latter and investigate the adiabatic exact-exchange functional, AEXX, which, for a two-electron system, is simply $v_{\text{xc}}^{\text{AEXX}}[n](\mathbf{r}, t) = -v_H[n](\mathbf{r}, t)/2$. In Fig. 6 we compare the adiabatically exact xc potential found in the previous section to AEXX, at the initial time. The undulations of the exact adiabatic xc potential that are missing in the AEXX represent correlation; they are relatively small in this particular case once added to the external potential, so we expect that AEXX dynamics fairly approximates the adiabatically exact dynamics in this situation at least for short times.

We now return to the error of not having the correct initial density (Sec. IV A).

In a usual TDDFT calculation, a ground-state DFT calculation is first performed and the orbitals from this are used to create the initial wavefunction. So we would start with the ground-state KS density of Fig. 2 except

here there is a further error that will be made, as an approximate ground-state xc functional is used instead of the exact one.

In Fig. 7 we plot the ground- and first-excited- KS orbitals from ground-state DFT calculations using EXX and LDA for the soft-Coulomb helium atom, and compare to the exact KS orbitals. We also plot, for completeness, the pair of orbitals found for this configuration that yield the exact *interacting* excited-state density, i.e. these are the exact orbitals which, when singly-occupied, make up the densities shown in Fig. 2.

If we first compare the approximate orbitals to the exact KS orbitals of the soft-Coulomb potential, we find both LDA and EXX perform very well, particularly for the ground-state orbital. Their ground-state KS potentials are however quite different: it is well known that the LDA potential is much too shallow, with a much too rapid exponential decay away from the nucleus, while the EXX is much closer to the exact, with the correct asymptotic decay. This is reflected in the first-excited orbital in LDA, which is more diffuse than EXX and the first-excited orbital of the exact soft-Coulomb KS potential. The asymptotic behavior will be important especially when we turn on an electric field, so we will (mostly) use the EXX orbitals to build our initial KS wavefunctions.

In the next section we will add the spin-symmetry-broken initial state (c) introduced in Section II to our investigations; while no longer a spin eigenstate like the exact case or Φ^* and Φ^{gs} , this still has the same total density as the exact system. We will simply construct this from the same EXX orbitals composing Φ^* , but will evolve the two orbitals using *different* xc potentials, v_{xc}^{\uparrow} and $v_{\text{xc}}^{\downarrow}$. For exact-exchange, we have $v_{\text{HXC}}^{\uparrow\downarrow}[n](x) = v_{\text{H}}[n^{\uparrow\downarrow}](x)$ for two electrons. We are however *not* doing spin-DFT since the individual spin-densities are not physical ones; we only ever consider their sum as observable. (Indeed, even the initial spin-densities are wrong). The point of considering such an initial state and dynamics is that, for two electrons, it is an example of dynamics in *orbital-specific* potentials, as would occur in generalized KS approaches [36–38]. Orbital-dependent functionals require an optimized effective potential approach to find a single potential for all the KS orbitals to live in. This procedure is numerically very intensive, so often a generalized KS approach is used, that relaxes the condition that all orbitals evolve under the same potential; moreover, the latter has shown to have certain advantages over the OEP in certain cases, e.g. better band-gaps. The interest in orbital-dependent functionals is that that they can work less hard to capture both spatially-non-local and time non-local- density-dependence since the orbitals themselves are non-local functionals of the density.

We note nevertheless that it can be shown there is no ISD for two-electron dynamics with spin-TDDFT; this follows straightforwardly generalizing the arguments of Ref. 27 to each spin-density. This is not the case for our

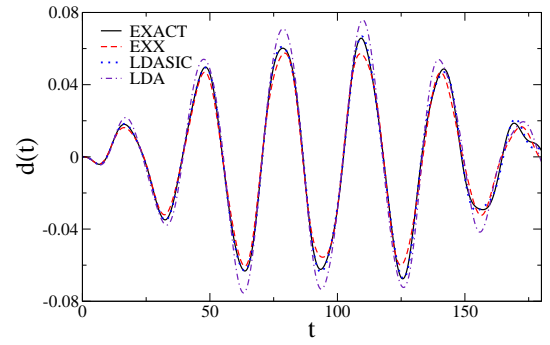


FIG. 8: The exact dipole moment and those from TDDFT calculations starting in the self-consistent ground-state KS wavefunction and propagated with the corresponding adiabatic approximation, all under the influence of the electric field described in the text.

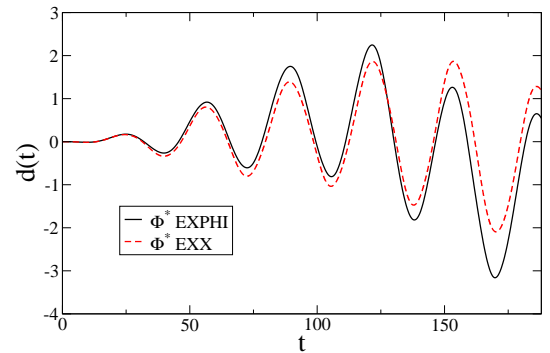


FIG. 9: The dipole moments when beginning in Φ^* composed of EXX orbitals (dashed line) and the exact orbitals of Sec. IV A (solid line) in the electric field (see text).

spin-broken case, however, as here we are *not* attempting to reproduce the exact spin-densities but rather the total density evolution; only $n(\mathbf{r}) = n_{\uparrow} + n_{\downarrow}$ will be considered meaningful.

Having delineated and explored the three possible sources of error in an adiabatic TDDFT calculation of excited state dynamics, we are now ready to run a typical adiabatic TDDFT calculation on our model systems, starting with our different choices of initial KS states, and compare with the exact result.

D. Propagation in an electric field

We simulate electric-field driven dynamics in the soft-Coulomb helium model, using adiabatic TDDFT. We apply a relatively weak oscillating electric field of amplitude 0.01au with an off-resonant frequency of 0.2a.u. We run for 6-cycles including a trapezoidal envelope consisting of a 2-cycle linear switch on and a 2-cycle switch off.

As a point of reference, we first look at the performance of TDDFT when starting in the *ground state*. We

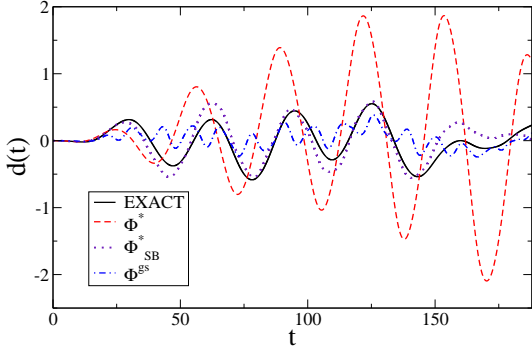


FIG. 10: The dipole moments for dynamics in the given electric field starting in the Φ^* , Φ_{SB}^* , Φ^{gs} initial KS wavefunctions and using AEXX, compared to exact.

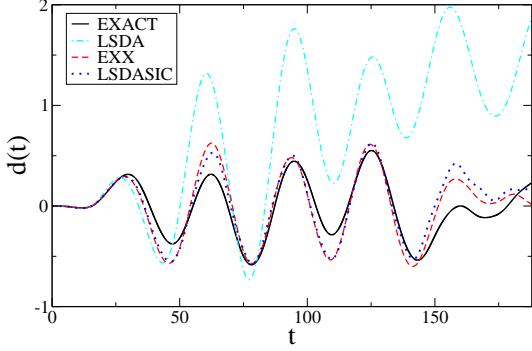


FIG. 11: Dynamics for the spin-broken case, Φ_{SB}^* , for different orbital-specific adiabatic functionals, EXX, LSDASIC, and LSDA, compared to the exact.

propagate the doubly-occupied EXX ground-state orbital in the electric field, using AEXX, and compare to the exact dynamics of the initial interacting ground-state. The resulting dipole moment is very accurate as can be seen in Fig. 8. In fact, almost exact dynamics can be achieved in this case with an adiabatic approximation: the same figure shows the result of using the adiabatic self-interaction corrected LDA approximation (LDASIC) to propagate the LDASIC ground-state orbital. The dipole moment lies practically on top of the exact curve. Including correlation in a self-interaction free functional therefore improves over exact exchange, but an adiabatic approximation is certainly adequate in this case. We also show for comparison the LDA result.

The adiabatic approximation is however not so rosy, as we shall see, in the case of an initially excited state. The initial interacting state is the first singlet excited state ($E = -1.705\text{au}$).

The typical TDDFT calculation will begin in an excited state determined by the orbitals of the corresponding ground-state KS system, but as discussed in Sec. IV A, this does not have quite the right density to start with. Since in our model system, we found an initial KS state of the correct density, we first check the

error that using the AEXX orbitals make. We plot in Fig. 9 the dipole moments for AEXX calculations starting in the Φ^* initial state with exact orbitals and with the ground-state EXX orbitals (i.e. using the solid and dotted orbitals of Figure 7 respectively). As

previously anticipated, the two calculations perform similarly, especially at shorter times.

At last we are ready to study the excited-state electron dynamics, using, as in practical calculations, an approximate ground-state KS potential (in this case EXX) to generate the orbitals composing the various initial state choices. In Fig. 10, we plot the dipole moment for each choice of initial state. The spin-broken-symmetry case gives the best dynamics; as mentioned earlier, functionals expressed directly in terms of instantaneous orbitals automatically contain time non-local and spatially-non-local density-information. In this particular case the orbital-specific EXX potentials, obtained from spin-scaling the (spin-restricted) AEXX potential, are self-interaction-free, while the latter is not for the case of the *excited* two-orbital singlet state.

Unlike in the propagation of the ground-state, adding correlation to the adiabatic potential does not significantly improve the results, as can be seen in Fig. 11; the symmetry-broken LSDASIC and EXX calculations are both off by roughly the same amount. Fig. 11 also shows the LSDA result, clearly worse than the others by comparison.

The Φ^* initial state has the correct spin symmetry and is closest in character to the true excited state, being a double Slater determinant. It gives better dynamics than the $\Phi^{gs}[n^*]$ initial state, whose dynamics are completely incorrect. This is consistent with the results in the previous sections. We can say with confidence that it is ISD, and its underlying static correlation that it causing poor dynamics for this doubly-occupied-singlet case.

We can understand the poor result for the initial state of the Eq. (8) form also by looking at the exact adiabatic xc potential and $v_{xc}[n^*, \Psi^*, \Phi^{gs}[n^*]](x)$, both shown in Fig. 4. This form treats the density as if it were a ground-state and uses one doubly occupied orbital, inversion of this orbital yields $v_s^{\text{adia-all}}[n](x)$, i.e. this is the potential in which the wavefunction is static at the initial time. However in a calculation using the adiabatic approximation, it will fall into a much deeper potential, drastically affecting its dynamics. Without the initial-state dependence of the xc potential giving a bump similar to Fig. 1, it will perform poorly.

V. MODEL LIH DYNAMICS

Our final example is perhaps the most topical one where the initial state is an excited one: coupled electron-ion dynamics after photo-excitation. The initial excitation is assumed to place the initial nuclear wavepacket on an excited potential energy surface, vertically up from its ground-state equilibrium. Field-free

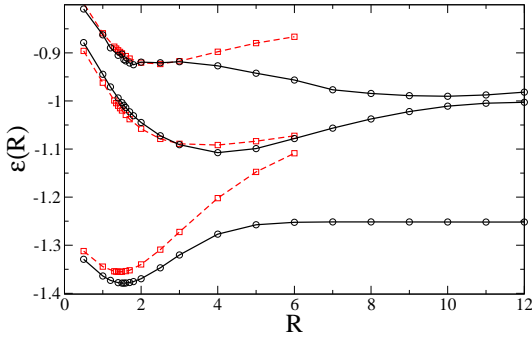


FIG. 12: The exact Born-Oppenheimer potential energy surfaces (solid lines) and the EXX KS Born-Oppenheimer surfaces (dashed lines). Note that due to degeneracy between the lowest two surfaces, these calculations cannot be converged for large values of R , the interatomic separation.

dynamics on the excited surface ensues; usually the nuclei are treated classically, coupled in either an Ehrenfest or surface-hopping scheme to the quantum electron dynamics. For Ehrenfest dynamics in the TDDFT framework [33], and the simplest type of surface-hopping [39], the electrons start in the KS excited-state obtained simply from promoting an electron from the highest occupied orbital in the ground-state KS configuration to a virtual orbital. This initial state is then evolved in the time-dependent external potential caused by the moving ions. The dynamics of the ions is given by simple Newtonian mechanics where the electronic system provides a force $\int n(\mathbf{r}, t) \nabla_R v_{\text{ext}}(\mathbf{r}; \{\mathbf{R}\})$, where $\{\mathbf{R}\}$ represent the nuclear coordinates. All the three errors mentioned earlier therefore raise their heads: the initial density is not that of the true excited state (even if the exact xc potential was used), an adiabatic approximation is used to propagate it, and this involves an approximate ground-state functional. It should be noted that in the more accurate surface-hopping method of Ref. [40], where correct TDDFT surfaces are used to provide the nuclear forces [41], the first problem does not arise; the method in fact circumvents having to define the electronic state.

We will use the parameters found in Ref. 42 for a one-dimensional two-electron lithium hydride model, where

$$v_{\text{ext}}(x) = -1/\sqrt{x^2 + 0.7} - 1/\sqrt{x^2 + 2.25} \quad (18)$$

and $v_{nn}(R) = -1.0/\sqrt{R^2 + 1.95}$. We integrate Newton's equations of motion using the leapfrog algorithm, and for simplicity, we use the same time step for both electrons and ions.

The Born-Oppenheimer potential energy surfaces are shown in Fig. 12 for both the exact system and those of the bare KS system calculated within spin restricted EXX.

The ground state surface has a minimum at $R = 1.55$, whereas the EXX has the gs equilibrium at $R = 1.45$.

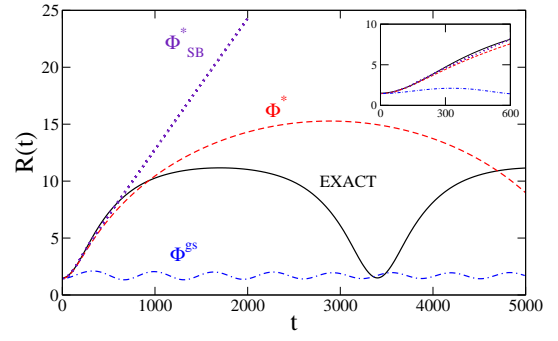


FIG. 13: The interatomic distance, $R(t)$, for Ehrenfest dynamics starting in the first excited-state and propagated freely. The various KS initial wavefunctions (Φ^* , Φ_{SB}^* , Φ^{gs}) are propagated with the adiabatic exact exchange approximation. Inset: short-time dynamics for the various initial states.

Near equilibrium the surfaces are somewhat similar. The spin-restricted EXX surfaces however encounter the well-known fractional charge problem as R increases, with the calculations becoming extremely difficult to converge and the lowest two surfaces collapsing onto each other. In the exact surface, an avoided crossing can be seen between the ground and first excited state around $R = 4$, where the latter establishes ionic character, eventually decaying as $-0.896 - 1/x$, while the neutral dissociation curve flattens out. In fact there are multiple avoided crossings at larger distances, the next being around $R = 10$. Unrestricted EXX calculations break the spin-symmetry of the true ground-state at a critical separation, but describe dissociation and the shape of the potential energy surfaces at larger distances qualitatively [43, 44].

We vertically excite the system at the ground-state equilibrium geometry into the first excited singlet state and then begin the propagation with the initial nuclear momentum chosen as zero. In Fig. 13, we show the internuclear separation as a function of time for our three choices of initial states, calculated within EXX. For Φ^* we make the usual practise of taking ϕ_0 in Eqs. 7 and 10 as the HOMO and ϕ_1 as the LUMO; likewise for the spin-symmetry-broken version Φ_{SB}^* . The density of this state n^* is then used to define the doubly-occupied orbital in the SSD state $\Phi^{\text{gs}}[n^*]$ (Eq. 8).

For this particular system, the exact system remains on the first excited surface; the nuclear coordinate oscillates between the turning points at $R = 1.5$ and $R = 11.65$. The ground state Φ^{gs} completely fails to capture this behavior, making only very small oscillations around its initial position. The excited states Φ^* and Φ_{SB}^* show reasonable agreement for short times, with the spin-broken state once again edging out the other. For longer times however, the spin-broken state is dramatically wrong, yielding nuclei moving away from each other with constant speed. The excited state Φ^* shows behavior more qualitatively exact but, because of the deviation of its potential energy curve compared to

the exact one, the oscillation period is quite wrong.

The conclusions regarding ISD in this example, at least at short times, are consistent with the results throughout this paper and support the idea that when using an adiabatic approximation choosing a KS initial-state with a configuration close to that of the exact interacting initial state yields the better result. However, the behavior at longer times in this problem highlights, above all, the need for accurate ground-state functionals: EXX produces poor nuclear dynamics when Φ^* is chosen as the KS state primarily because the shape of its potential energy surfaces is wrong – the ground state as well as the excited state ones. Any adiabatic approximation that does not have strong correlation will not perform well. Despite giving improved potential energy surfaces, the spin-broken EXX approach fails for dynamics for longer times. We believe this is because as the molecule dissociates, symmetry-breaking localizes each electron on one nucleus or the other, with each evolving according to a different xc potential; each atom sees just a neutral atom, leading to a net zero potential, and a constant velocity (somewhat as if the molecule was dissociating on the ground-state surface). It should be noted that the spin-broken solution is not evolving on the spin-broken PES. e.g. even at the initial time, at the equilibrium geometry there is no symmetry-breaking in a spin-unrestricted approach, so the spin-broken surface is on top of the spin-restricted surface showed in the figure. However the spin-broken wavefunction (c) is evolved using different potentials for each orbital, unlike the evolution dictated by either the spin-restricted EXX surface or the unrestricted EXX (the symmetry-breaking point occurs around $R = 2.5$).

VI. CONCLUSIONS AND OUTLOOK

Until relatively recently, ISD fell in the realm of a theoretical curiosity, but due to an increasing number of topical applications beginning with the system not in its ground-state, ISD is now also of much practical concern. Almost all calculations today use adiabatic functionals that neglect the ISD that the exact functionals are known to have.

By considering several choices of initial KS states when the initial interacting state is excited, we explored the effect of ISD on dynamics in several exactly-solvable model systems and the performance of the adiabatic approximation. We noted there are three sources of error: excited KS initial states do not have the same density as the corresponding true excited states even when the exact functional is used, the use of the adiabatic approx-

imation to propagate the initial state, and the ground-state functional generating the adiabatic approximation itself being approximate. By separating these errors from each other, we were able to properly assign how badly they impacted the dynamics in model systems, allowing us to see the effect of ISD more clearly.

When the initial KS state has a configuration that is significantly different than the true state, the adiabatic approximation fails severely – even for non-interacting electrons, where there is a significant error that can be interpreted as a static correlation effect. The optimal choice for the KS initial state is one whose configuration is most similar to the true excited state; this is in fact the usual practise in recent calculations (e.g. Ref. [33]). The error in using an adiabatic xc functional to propagate such a state, however, is significantly larger than the error the same functional produces when describing the propagation of an initial true ground-state, as demonstrated by the model soft-Coulomb helium atom example. For two electrons, the spin-broken initial KS state, with the two orbitals evolved under different spin-decomposed potentials (depending on the instantaneous spin-densities), often appeared to be the best choice, suggesting that orbital-specific potentials (allowed by the generalized KS scheme) could be a useful future avenue of research for TDDFT. However, how to obtain such potentials in a general N -electron case is not obvious (at least without the need for empirical parameters). Generally, orbital-dependent functionals treated within the OEP may be promising for these problems where memory-(of the density)-dependence, including ISD at the KS level only, is naturally captured by the KS orbitals; again, devising suitable orbital-dependent functionals with the appropriate ISD is a direction for future research.

The example of coupled electron-nuclear dynamics in the model LiH molecule, although supporting the earlier results of the optimal choice of a KS initial state, above all, highlighted the need for more accurate ground-state functional approximations for dissociation.

We do not provide in this work an approximation that includes ISD, both of the true interacting state and the KS state; this is likely a difficult task. But what is clear from the results in this paper, and the stage of the field, is that now is the right time to address this issue.

Acknowledgments Financial support from the National Science Foundation (CHE-1152784), and a grant of computer time from the CUNY High Performance Computing Center under NSF Grants CNS-0855217 and CNS-0958379, are gratefully acknowledged.

-
- [1] E. Runge and E.K.U. Gross, Phys. Rev. Lett. **52**, 997 (1984).
 - [2] *Fundamentals of Time-Dependent Density Functional Theory*, (Lecture Notes in Physics 837), eds. M.A.L. Marques,

- N.T. Maitra, F. Nogueira, E.K.U. Gross, and A. Rubio, (Springer-Verlag, Berlin, Heidelberg, 2012).
- [3] P. Hohenberg and W. Kohn, Phys. Rev. **136**, B 864 (1964).

- [4] W. Kohn and L.J. Sham, Phys. Rev. **140**, A 1133 (1965).
- [5] W. Kohn, Rev. Mod. Phys. **71**, 1253 (1999).
- [6] E.K.U. Gross and W. Kohn, Phys. Rev. Lett. **55**, 2850 (1985); **57**, 923 (1986) (E).
- [7] J.F. Dobson, Phys. Rev. Lett. **73**, 2244 (1994).
- [8] G. Vignale and W. Kohn, Phys. Rev. Lett. **77**, 2037 (1996).
- [9] J.F. Dobson, M.J. B  nner, and E.K.U. Gross, Phys. Rev. Lett. **79**, 1905 (1997).
- [10] G. Vignale, C.A. Ullrich, and S. Conti, Phys. Rev. Lett. **79**, 4878 (1997).
- [11] I.V. Tokatly and O. Pankratov, Phys. Rev. B **67**, 201103 (2003).
- [12] Y. Kurzweil and R. Baer, J. Chem. Phys. **121**, 8731 (2004).
- [13] H.O. Wijewardane and C.A. Ullrich, Phys. Rev. Lett. **100**, 056404 (2008).
- [14] I.V. Tokatly in *Fundamentals of Time-Dependent Density Functional Theory, (Lecture Notes in Physics 837)*, eds. M.A.L. Marques, N.T. Maitra, F. Nogueira, E.K.U. Gross, and A. Rubio, (Springer, Berlin, Heidelberg, 2012).
- [15] N.T. Maitra, F. Zhang, R.J. Cave and K. Burke, J. Chem. Phys. **120**, 5932 (2004).
- [16] M. Gatti, V. Olevano, L. Reining, and I.V. Tokatly, Phys. Rev. Lett. **99**, 057401 (2007).
- [17] E. Penka Fowe and A. D. Bandrauk, Phys. Rev. A **84**, 035402 (2011).
- [18] E. Tapavicza, I. Tavernelli, U. Rothlisberger, C. Filippi, and M. E. Casida, J. Chem. Phys. **129**, 124108 (2008).
- [19] J. Gavnholt, A. Rubio, T. Olsen, K. S. Thygesen, and J. Schi  tz, Phys. Rev. B **79**, 195405 (2009).
- [20] I. DAmico and G. Vignale, Phys. Rev. B **59**, 7876 (1999).
- [21] P. Hessler, N.T. Maitra, and K. Burke, J. Chem. Phys. **117**, 72 (2002).
- [22] N. T. Maitra and K. Burke, Chem. Phys. Lett. **359**, 237 (2002).
- [23] C.A. Ullrich, J. Chem. Phys. **125**, 234108, (2006).
- [24] J. I. Fuks, N. Helbig, I. V. Tokatly, and A. Rubio, Phys. Rev. B. **84**, 075107 (2011).
- [25] M. Thiele, E.K.U. Gross, S. Kummel, Phys. Rev. Lett. **100**, 153004 (2008).
- [26] R. Baer, J. Mol. Struct.: THEOCHEM **914**, 19 (2009).
- [27] N.T. Maitra and K. Burke, Phys. Rev. A **63**, 042501 (2001); **64** 039901(E).
- [28] N.T. Maitra, K. Burke, and C. Woodward, Phys. Rev. Lett. **89**, 023002 (2002).
- [29] R. van Leeuwen, Phys. Rev. Lett. **82**, 3863 (1999).
- [30] I. Dreissigacker and M. Lein, Chem. Phys. **391**, 143 (2011).
- [31] J. Javanainen, J.H. Eberly, and Q. Su, Phys. Rev. A **38**, 3430 (1988); W.-C. Liu, J.H. Eberly, S.L. Haan, and R. Grobe, Phys. Rev. Lett. **83**, 520 (1999); D.M. Villeneuve, M.Y. Ivanov, and P.B. Corkum, Phys. Rev. A. **54**, 736 (1996); A. Bandrauk and H. Ngyuen, Phys. Rev. A. **66**, 031401(R) (2002); M. Lein, E.K.U. Gross, and V. Engel, Phys. Rev. Lett. **85**, 4707 (2000).
- [32] A. Castro, H. Appel, M. Oliveira, C.A. Rozzi, X. Andrade, F. Lorenzen, M.A.L. Marques, E.K.U. Gross, and A. Rubio, Phys. Stat. Sol. B **243**, 2465 (2006).
- [33] I. Tavernelli, U.F. R  hrig, and U. Rothlisberger, Mol. Phys. **103**, 963 (2005).
- [34] R. Gaudoin and K. Burke, Phys. Rev. Lett. **93**, 173001 (2004).
- [35] K. Peirs, D. Van Neck, and M. Waroquier, Phys. Rev. A **67**, 012505 (2003).
- [36] A. Seidl, A. G  rling, P. Vogl, J.A. Majewski, and M. Levy, Phys. Rev. B **53**, 3764 (1996).
- [37] S. K  mmel in *Fundamentals of Time-Dependent Density Functional Theory, (Lecture Notes in Physics 837)*, eds. M.A.L. Marques, N.T. Maitra, F. Nogueira, E.K.U. Gross, and A. Rubio, (Springer, Berlin, Heidelberg, 2012).
- [38] A. G  rling and M. Levy, J. Chem. Phys. **106**, 2675 (1997).
- [39] C.F. Craig, W.R. Duncan, and O.V. Prezhdo, Phys. Rev. Lett. **95**, 163001 (2005).
- [40] E. Tapavicza, I. Tavernelli, and U. Rothlisberger, Phys. Rev. Lett. **98**, 023001 (2007).
- [41] N. T. Maitra, J. Chem. Phys. **125**, 014110 (2006).
- [42] D.G. Tempel, T.J. Mart  nez, and N.T. Maitra, J. Chem. Theory and Comput., **5**, 770 (2009).
- [43] M.E. Casida, F. Gutierrez, J. Guan, F-X. Gadea, D. Salahub, and J-P. Daudey, J. Chem. Phys. **113**, 7062 (2000).
- [44] J.I. Fuks, A. Rubio, and N.T. Maitra, Phys. Rev. A **83**, 042501 (2011).